33rd Annual International Conference of the IEEE EMBS
Boston, Massachusetts USA, August 30 - September 3, 2011

Influence of the Multisine Excitation Amplitude Design for Biomedical Applications using Impedance Spectroscopy

Benjamin Sanchez, Ramon Bragos and Gerd Vandersteen

Abstract— **Electrical Impedance Spectroscopy (EIS) is a powerful tool to collect data from many biological materials in a wide variety of applications. Body composition fluid or tissue and organ state monitoring are just some examples of these applications. While the classical EIS is based on frequency sweep, the EIS technique using broadband excitations allows to acquire simultaneous impedance spectrum data. The strength and weakness of broadband EIS relies on the fact that it enables multiple Electrical Bio-Impedance (EBI) data collection in a short measuring time but at the cost of losing impedance spectrum accuracy. In general, there is a relationship between the broadband excitation time/frequency properties and the final EBI's accuracy obtained. This paper studies the influence of the multisine broadband excitation amplitude's design over the EBI accuracy by means of the resultant Noise-to-Signal Ratio (NSR) obtained when measuring with a custom impedance analyzer. Theory has been supported by a set of validation experiments.**

I. Introduction

Electrical Impedance Spectroscopy (EIS) is a technique extensively used in many electrochemical and biomedical applications for characterizing electrically the passive electrical properties of materials. Often, the EIS is based on time limited voltage and current measurements, which are then Fourier-transformed to the frequency domain for determining the frequency response. Since the biological objects are highly sensitive to the electric field applied, this time - frequency transformation is only valid when the system behaves linear and time invariant. In practice, these restrictions are put in practice by limiting the excitation peak value in order to ensure a system linear response. There are many different types of electrical stimuli used in EIS that may be applied to the system and result in a measured time-varying voltage $v(t)$. The most common among all the approaches to EIS experiments is the application of a single-frequency sinusoidal current stimulus $i(t)$. The impedance spectrum then can be determined by sweeping the exciting frequency in the range of interest and measuring the phase shift and amplitude of the resulting voltage of the response at each frequency. The major advantage of this approach relies on the fact that high Signal-to-Noise Ratio (SNR) at the excited frequencies is obtained but at the price of increasing the measuring time.

A second approach consists on applying a broadband excitation with the energy content at the whole frequency range of interest. The resulting frequency response can be found by means of spectral analysis using the Fast Fourier Transform (FFT). In contrast to the frequency sweep approach, the broadband EIS technique offers the advantage of simultaneous impedance spectrum data collection. While the frequency sweep must wait until the transient expires for all the measured frequencies, the broadband EIS waits just the initial transient. As a consequence of the measuring time reduction, the broadband excitations are suitable in those applications where high throughput real-time data demands and monitoring are required. A practical example is presented in [1], where there is a low cost microfluidic device system implementation for determining the electrical properties of single cells, by exciting within 1ms measuring time using Maximum Length Binary Sequences (MLBS). Another custom impedance analyzer implementation is presented in [2], which combines multisine excitation and Pseudo-Random Binary Sequences (PRBS) from LF to 5 GHz. Finally, the custom multisine impedance analyzer presented in [3] was used for *in-vivo* cardiovascular system characterization during an ischemic process. However, the weakness of such kind of broadband EIS measuring techniques is its intrinsic loss of accuracy. At the end, the final measuring time will be determined by the minimum EBI accuracy required.

The aim of this work is to compare different amplitude broadband multisine excitations to determine the strengths and weaknesses of each one in order to obtain the most accurate impedance spectrum. This study has been done based on the theoretical impedance spectrum dispersion and variance and verified with experimental data from multifrequency impedance measurements carried out with a custom PXI based impedance analyzer.

II. Broadband EIS using multisine excitation

A real multisine excitation $u[n]$ consists of a sum of of M sines (or cosines), each one with its own phase φ_m given by:

$$u[n] = \sum_{m=1}^{M} a_m \cos[2\pi f_m n + \varphi_m] \qquad (1)$$

where a_m are the multisine fundamental's amplitudes and f_m are the exciting frequencies. The Crest Factor of an excitation $u[n]$ is a metric that is defined as the ratio of its peak value

This work has been supported in part by the Spanish Ministry MICINN SAF2008-05144-C02-02, 080331 from Fundació La Marató de TV3, by the REDINSCOR, by the Fund for Scientific Research (FWO-Vlaanderen), by the Flemish Government (Methusalem), and by the Belgian Government through the Interuniversity Poles of Attraction (IAP VI/4) Program.

G. Vandersteen is with the ELEC Department, Vrije Universiteit Brussels (VUB), Brussels, 1050, BELGIUM.

B. Sanchez and R. Bragos are with the Department of Electrical Engineering, Technical University of Catalonia (UPC), Barcelona, 08034, SPAIN. benjamin.sanchez@upc.edu

l_∞ and its root mean square value (rms) l_2. Hence,

$$CF(u) = \frac{l_\infty(u)}{l_2(u)} = \frac{\max_{n\in[0,N-1]} |u[n]|}{\sqrt{\frac{1}{N}\sum_{n=0}^{N-1} |u[n]|}} \quad (2)$$

The Crest Factor allows to determine how the energy is employed by the excitation to inject a given power level into the system, and this will vary as a result of the excitation design. The multisine rms value is independent of the φ_m phases while its peak value is highly sensitive to them. The maximal peak l_∞ can be significantly compressed by the proper choice of the phases φ_m, which is the same as minimizing the Crest Factor. Then, the lower Crest Factor, the more energy is transferred to the system for a given input dynamic range resulting into a maximal Signal-to-Noise Ratio (SNR).

III. Case of study: multisine amplitude power spectrum

In general, measuring a system is a two-step process. First measurements are usually carried out using a full grid multisine excitation in order to obtain a general overview of the system and to obtain a preliminary model for describing the data. In this case, the Crest Factor can be efficiently reduced by the use of the Newman phases [4], which work well for unitary amplitudes (see Fig. 1). Then, the frequency response function of the system is used within the excitation signal design process to improve the excitation time - frequency features with the goal of increasing the frequency response accuracy for a second step of measurements.

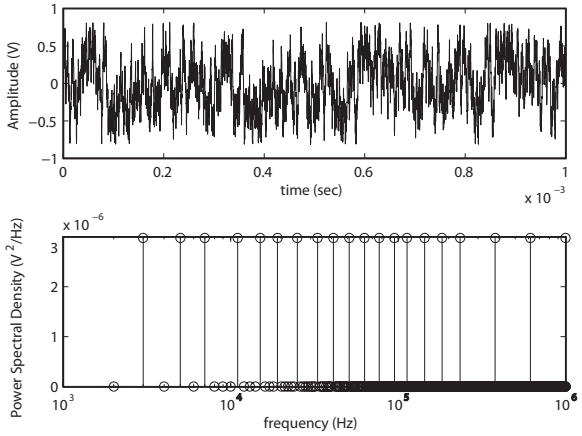

Fig. 1. Multisine time (top) and its power spectral density (bottom) with a flat amplitude power spectrum (CF=2.3).

In this second step, the excitation can be designed to e.g. decrease the uncertainty of the EBI spectrum data at those frequencies with low SNR. This is the case of EBI, which usually presents a strong and weak response at low and high frequencies respectively. To design the optimal multisine excitation, Popkirov *et al* proposed in [5] that the multisine fundamental's amplitudes should be designed according to the impedance spectrum magnitude measured $a_m = k|Z(f_m)|$ (see Fig. 2), where f_m are the exciting frequencies and k is a gain factor.

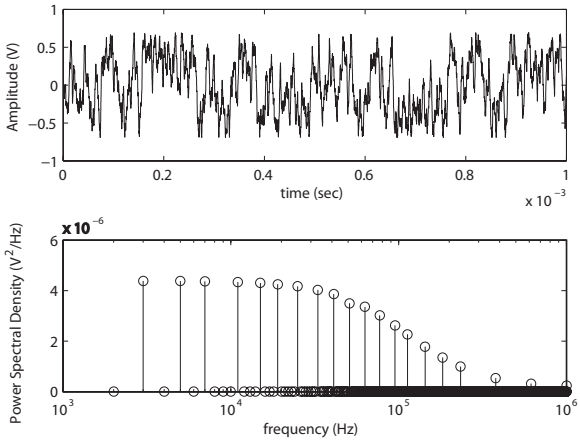

Fig. 2. Multisine time (top) and its power spectral density (bottom) with the amplitudes following the impedance spectrum (CF=1.95).

Nevertheless, a time/frequency optimization process is needed in order to design the optimal multisine excitation, where some previous knowledge and information of the system to be measured is assumed to be known. We will refer to the optimal multisine as the multisine described in [6] shown in Fig. 3. This multisine excitation was designed to minimize the maximum value of the EBI dispersion function $\upsilon(\theta, S_u, \omega)$ for a discrete set of the exciting frequencies f_m given by:

$$\upsilon(\theta, S_u, \omega) = trace\left\{ \left[\overline{M}(\theta, S_u)\right]^{-1} \widetilde{M}(\theta, \omega) \right\} \quad (3)$$

where $S_u(\omega)$ is the multisine spectral density and $\widetilde{M}(\theta,\omega)$ refers to the single frequency Electrical Bioimpedance Fisher Information matrix described in [6]. The EBI dispersion $\upsilon(\theta, S_u, \omega)$ is defined as a normalized variable describing the uncertainty on the system defined by the trace of the resulting matrix of the complete Electrical Bioimpedance Fisher Information matrix inverse $\overline{M}(\theta, S_u)$ with the information matrix corresponding to a single frequency input $\widetilde{M}(\theta,\omega)$.

A property of the dispersion function $\upsilon(\theta, S_u, \omega)$ is that it can be related to the variance of the EBI spectrum $\sigma_Z^2(\omega)$ by means of the additive input with respect to their input/output variances σ_u and σ_y according to the following equation:

$$\sigma_Z^2(\omega) = \upsilon(\theta, S_u, \omega)\left(\sigma_U^2(\omega)|Z(\omega)|^2 + \sigma_Y^2(\omega)\right) \quad (4)$$

Then, the multisine spectral density $S_u(\omega)$ can be designed to minimize the maximum value of the EBI dispersion function $\upsilon(\theta, S_u, \omega)$, which will lead to minimize the maximum value of the EBI spectrum variance $\sigma_Z^2(\omega)$. The following results have been obtained solving Eq.3 and Eq.4 considering an EBI system described by the continuous model $Z(s)$ given by:

$$Z(s) = \frac{\mathrm{R}_e R_i C_m s + \mathrm{R}_e}{(\mathrm{R}_e + R_i) C_m s + 1} \quad (5)$$

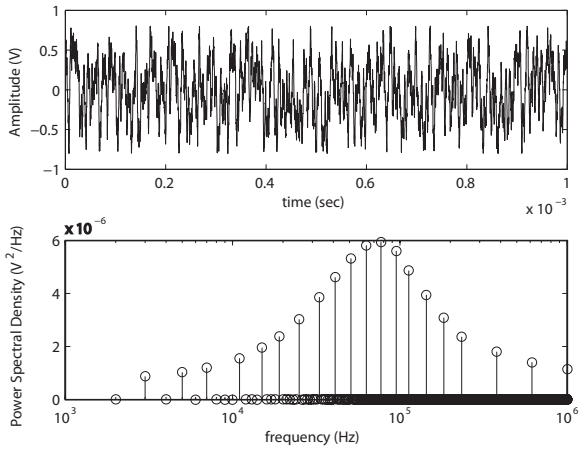

Fig. 3. Optimal multisine (top) and its power spectral density (bottom) (CF=2.27).

where the parameters are set to R_e=30 Ω, R_i=120 Ω and C_m=10 nF. Its frequency response is shown in Fig. 4. This impedance relaxation corresponds to a series R_iC_m circuit in parallel with R_e, which models the myocardial tissue impedance in the first acute phase of ischemia [3]. Designing

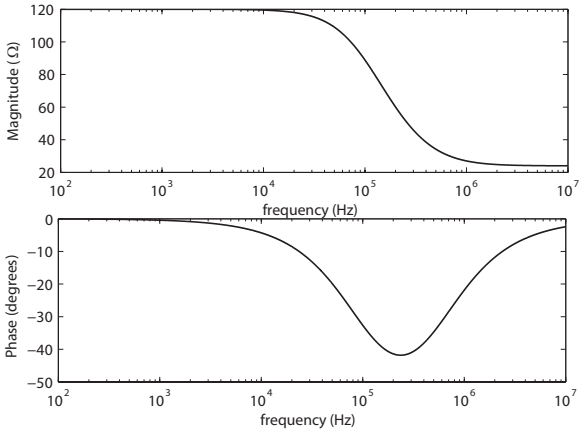

Fig. 4. Impedance frequency response function.

the multisine amplitudes following the impedance spectrum as proposed in [5] helps to reduce the scattering of the impedance spectrum at low frequencies significantly at the cost of getting dispersive results around the central frequency (see Fig. 5 top). However, the optimal multisine obtains good results at the frequencies where it has been designed to decrease the dispersion. The flat multisine equally distributes the energy in all the exciting frequencies, resulting in a dispersion that is in the middle of both previous designs.

The effect over the EBI spectrum variance σ_Z^2 (see Eq.4) is shown in Fig. 5 (bottom) when exciting the system with the amplitudes following the impedance spectrum, which is much better at low frequencies while the remaining impedance points suffer from an accuracy loss close to the characteristic frequency of the relaxation. In contrast to this, the optimal amplitude spectrum performs much better close to the central frequency but the accuracy at low frequencies is a little bit compromised. In general, the flat amplitude multisine is a balance at all the excited frequencies.

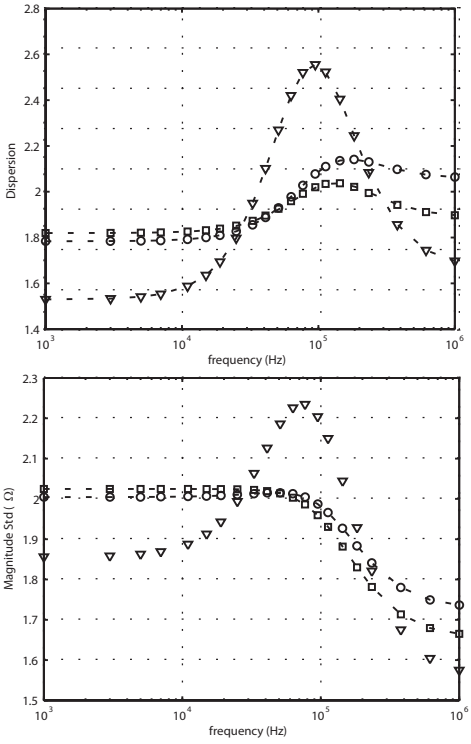

Fig. 5. EBI spectrum dispersion (see Eq.3) with a multisine power spectrum flat (circle), following impedance spectrum (triangle) and optimal (square) (top) and the EBI spectrum variance (see Eq.4) (bottom)

IV. Experimental Results

The multisine excitations described in section III have been tested on a custom multifrequency impedance analyzer built around a PXI system from National Instruments. The system includes an embedded dual-core controller PXIe-8130, a 2 channel high-speed digitizer card PXIe-5122 (100Ms/s, 64MB/channel, 14bits) and an arbitrary waveform card PXI-5422 (200Ms/s, 32MB, 16 bits). A dummy RC cell was implemented according to the parameters described in Eq.5. All measurements shown Fig. 6 were done using a custom 4 wire front end and they were compared to the measurements performed using an HP4294 impedance analyzer.

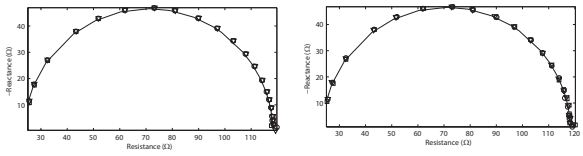

Fig. 6. Impedance plot with 1 V_p (left) and 25 mV_p (right) flat (circle), following the impedance spectrum (triangle) and optimal (square) amplitude multisine excitations and HP4294 (solid line). The resultant impedance spectrum Noise-to-Signal Ratio is shown in Fig.7.

The impedance spectrum Z_k^0 shown in Fig. 6 is the mean impedance spectrum magnitude determined at exciting

frequencies k by applying the classical spectral analysis based on cross and auto power spectrum using a rectangular window after averaging $M = 10$ periods of the current $i(t)$ and voltage $v(t)$ signals. Both signals were sampled at 20 MHz and measured with an integer number of cycles for each period. The EBI spectrum variance $\sigma^2_{Z_k}$ has been calculated according to the Eq.6 [7].

$$\begin{aligned} Z_k^0 &= \tfrac{1}{M}\sum_{n=1}^{M} Z_k^n \\ \sigma^2_{Z_k} &= \frac{|Z_k^0|^2}{M}\left(\frac{\sigma^2_{I_k}}{|I_k^0|^2} + \frac{\sigma^2_{V_k}}{|V_k^0|^2} - 2\Re e\left(\frac{\sigma^2_{V_k I_k}}{I_k^0 V_k^0}\right)\right) \end{aligned} \tag{6}$$

where I_0, σ_I^2 and V_0, σ_V^2 correspond to the mean spectrum magnitude and the variance of Fourier transformed coefficients from the current and voltage signals given by:

$$\begin{aligned} I_k^0 &= \tfrac{1}{M}\sum_{n=1}^{M} I_k^n, \quad \sigma^2_{I_k} = \tfrac{1}{M-1}\sum_{n=1}^{M}\left(I_k^n - I_k^0\right)^2 \\ V_k^0 &= \tfrac{1}{M}\sum_{n=1}^{M} V_k^n, \quad \sigma^2_{V_k} = \tfrac{1}{M-1}\sum_{n=1}^{M}\left(V_k^n - V_k^0\right)^2 \\ \sigma^2_{V_k I_k} &= \tfrac{1}{M-1}\sum_{n=1}^{M}\left(V_k^n - V_k^0\right)\left(I_k^n - I_k^0\right)^* \end{aligned} \tag{7}$$

Finally, the impedance spectrum NSR is defined as the ratio between the EBI impedance spectrum variance $\sigma^2_{Z_k}$ and the mean EBI impedance spectrum magnitude $|Z_k^0|^2$ given in Eq.6. Fig. 7 (top) shows the results obtained for multisine's peak amplitude limited to 1 V_p. The Popkirov *et al* proposal is specially good at low frequencies because more energy is applied. As a result of this, the variance dramatically increases as the frequency increases. The optimal multisine still obtains lower variance at those frequencies close to the central frequency of the impedance relaxation, while the variance at low and high frequencies is a little bit increased. Fig. 7 (bottom) shows the results when exciting with a 25 mV_p amplitude limited multisine. In this case, the EBI spectrum variance increases about 20 dB with respect to the 1 V_p because of the lower SNR measuring conditions. However, the trends are almost the same: the multisine excitation designed with amplitudes following the impedance spectrum obtains low EBI variance at low frequencies than higher frequencies. The optimal multisine still performs better than the rest at these exciting frequencies where it has been designed, with an improvement of about 5 dB with respect to the other multisine designs. The flat multisine obtains a NSR with good results at all the frequencies.

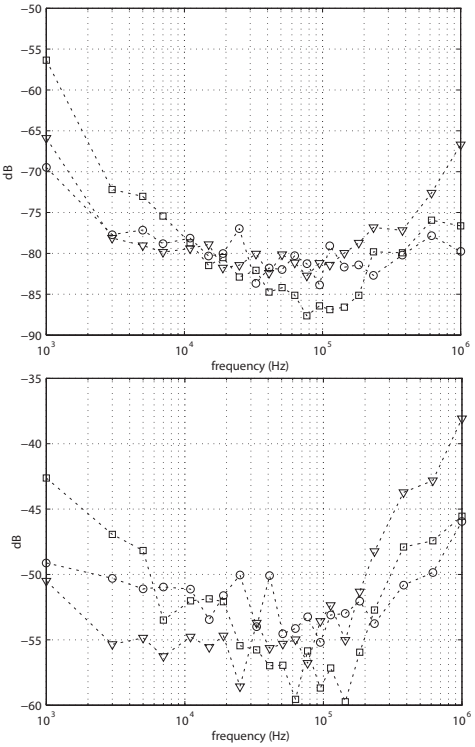

Fig. 7. Impedance spectrum NSR under two different scenarios: excitations limited to 1 V_p (top) and 25 mV_p (bottom) with a flat (circle), following the impedance spectrum (triangle) and optimal (square) multisine amplitude designs.

V. Conclusions

Multisine excitations with an amplitude spectrum that follows the impedance spectrum results in poor SNR at high frequencies. The reported results state that the major part of the impedance dispersion is close to the central frequency of the impedance relaxation. Focusing the excitation energy at low frequency is not therefore a good option since it does not help to reduce the impedance spectrum uncertainty at all the remaining frequencies. In general, multisine excitation should be designed to minimize the maximum value of the impedance spectrum variance, which is the only way to obtain the best accurate model parameters.

References

[1] H. Morgan, T. Sun, D. Holmes, S. Gawad, and N. Green, "Single cell dielectric spectroscopy," *Journal of Physics D: Applied Physics*, vol. 40, no. 1, pp. 61–70, Jan. 2007. [Online]. Available: http://stacks.iop.org/0022-3727/40/i=1/a=S10?key=crossref.78df0f3cceb28afa2f0cc517d7931f53

[2] T. Nacke, A. Barthel, J. Friedrich, M. Helbig, J. Sachs, M. Schäfer, P. Peyerl, and U. Pliquett, "A new hard and software concept for impedance spectroscopy analysers for broadband process measurements," *International Federation for Medical and Biological Engineering*, vol. 17, pp. 194–197, 2007. [Online]. Available: http://dx.doi.org/10.1007/978-3-540-73841-1_52

[3] R. Bragos, R. Blanco-Enrich, O. Casas, and J. Rosell, "Characterisation of dynamic biologic systems using multisine based impedance spectroscopy," *IEEE Proceedings on Instrumentation and Measurement Technology Conference*, no. 1, pp. 44–47, 2001. [Online]. Available: http://ieeexplore.ieee.org/lpdocs/epic03/wrapper.htm?arnumber=928785

[4] E. Beller and D. J. Newman, "An L1 Extremal Problem for Polynomials," *Proceedings of the American Mathematical Society*, vol. 29, no. 3, pp. 474–481, 1971.

[5] G. S. Popkirov and F. Schindler, "Optimization spectroscopy of the perturbation signal for electrochemical in the time domain impedance," *Reviews in Scientific instruments*, vol. 64, no. 11, pp. 3111–3115, 1993.

[6] B. Sanchez, G. Vandersteen, R. Bragos, and J. Schoukens, "Optimal multisine excitation design for broadband Electrical Impedance Spectroscopy," submitted.

[7] J. Schoukens, G. Vandersteen, K. Barbé, and R. Pintelon, "Nonparametric Preprocessing in System Identification: a Powerful Tool," *European Journal of Control*, vol. 3-4, pp. 260–274, 2009.